PROCEEDINGS OF SCIENCE

Nonlocal PNJL models and heavy hybrid stars

David Blaschke*, **David E. Alvarez Castillo**†
Institute for Theoretical Physics, University of Wrocław, Wrocław, Poland
Bogoliubov Laboratory for Theoretical Physics, JINR Dubna, Russia
E-mail: blaschke@ift.uni.wroc.pl, alvarez@ift.uni.wroc.pl

Sanjin Benić
Physics Department, Faculty of Science, University of Zagreb, Zagreb 10000, Croatia
E-mail: sanjinb@phy.hr

Gustavo Contrera
CONICET, Rivadavia 1917, 1033 Buenos Aires, Argentina
Gravitation, Astrophysics and Cosmology Group, Facultad de Ciencias Astronómicas y Geofisicas, Universidad Nacional de La Plata, La Plata, Argentina
E-mail: guscontrera@gmail.com

Rafał Łastowiecki
Institute for Theoretical Physics, University of Wrocław, Wrocław, Poland
E-mail: lastowiecki@ift.uni.wroc.pl

Nonlocal PNJL models allow for a detailed description of chiral quark dynamics with running quark masses and wave function renormalization in accordance with lattice QCD (LQCD) in vacuum. Their generalization to finite temperature T and chemical potential μ allows to reproduce the μ-dependence of the pseudocritical temperature from LQCD when a nonvanishing vector meson coupling is adjusted. This restricts the region for the critical endpoint in the QCD phase diagram and stiffens the quark matter equation of state (EoS). It is demonstrated that the construction of a hybrid EoS for compact star applications within a two-phase approach employing the nonlocal PNJL EoS and an advanced hadronic EoS leads to the masquerade problem. A density dependence of the vector meson coupling is suggested as a possible solution which can be adjusted in a suitable way to describe hybrid stars with a maximum mass in excess of 2 $M_\odot$ with a possible early onset of quark deconfinement even in the cores of typical ($M \sim 1.4\, M_\odot$) neutron stars.

Xth Quark Confinement and the Hadron Spectrum,
October 8-12, 2012
TUM Campus Garching, Munich, Germany

*Speaker.
†Instituto de Física, Universidad Autónoma de San Luis Potosí, San Luis Potosí, S.L.P. 78290, México

1. Introduction

The measurement of the high mass of $M = 1.97 \pm 0.04\ M_\odot$ for the pulsar PSR J1614-2230 [1] has reinforced the question whether the phase transition to hyperon matter [2] or to deconfined quark matter [3] in compact stars can be excluded (see, e.g., [4, 5, 6, 7, 8, 9, 10, 11, 12]).

In the present contribution, we want to discuss an answer to this question on the basis of a recently developed approach to quark matter within a nonlocal Nambu–Jona-Lasinio (NJL) model coupled to the Polyakov loop [13, 14, 15] (denoted here as "nl-PNJL") in its extension including wave function renormalization (WFR) [16, 17, 18] which goes far beyond the local PNJL models.

These models have been developed and tested against modern LQCD data in the finite temperature domain and at small chemical potentials where also results from LQCD within Taylor expansion techniques exist [19]. The extension of nl-PNJL models to the full QCD phase diagram poses a challenge [20, 21]. In particular their extension to the zero temperature case for studies of deconfinement in compact stars has so far been performed without WFR [22, 23]. The inclusion of the latter into these studies is a novelty on which we present first results in this contribution.

2. Nonlocal PNJL model

The Lagrangian for the $SU(2)_f$ nonlocal models, including vector channel interactions, is given by

$$\mathscr{L} = \bar{q}(i\not{D} - m_0)q + \mathscr{L}_{\rm int} + \mathscr{U}(\Phi)\ , \tag{2.1}$$

where q is the $N_f = 2$ fermion doublet $q \equiv (u,d)^T$, and m_0 is the current quark mass (we consider isospin symmetry, that is $m_0 = m_u = m_d$). The covariant derivative is defined as $D_\mu \equiv \partial_\mu - iA_\mu$, where A_μ are color gauge fields. The nonlocal interaction channels are given by

$$\mathscr{L}_{\rm int} = -\frac{G_S}{2}\Big[j_S(x)j_S(x) + j_P(x)j_P(x) - j_p(x)j_p(x)\Big] - \frac{G_V}{2} j_V(x)\, j_V(x), \tag{2.2}$$

where the nonlocal currents are

$$\begin{aligned} j_a(x) &= \int d^4z\, g(z)\, \bar{q}\left(x + \frac{z}{2}\right)\, \Gamma_a\, q\left(x - \frac{z}{2}\right)\ ,\ \ a = S, P, V\ ,\\ j_p(x) &= \int d^4z\, f(z)\, \bar{q}\left(x + \frac{z}{2}\right)\, \frac{i\overleftrightarrow{\not{\partial}}}{2\,\kappa_p}\, q\left(x - \frac{z}{2}\right)\ , \end{aligned} \tag{2.3}$$

with $\Gamma_a = (\Gamma_S, \Gamma_P, \Gamma_V) = (\mathbb{1}, i\gamma_5\vec{\tau}, \gamma_0)$ for scalar, pseudoscalar and vector currents respectively, and $u(x')\overleftrightarrow{\partial} v(x) = u(x')\partial_x v(x) - \partial_{x'} u(x') v(x)$. The functions $g(z)$ and $f(z)$ in (2.3) are nonlocal covariant form factors characterizing the corresponding interactions. The scalar-isoscalar current $j_S(x)$ will generate the momentum dependent quark mass in the quark propagator, while the "momentum" current, $j_p(x)$, will be responsible for a momentum dependent WFR of the propagator. Note that the relative strength between both interaction terms is controlled by the mass parameter κ_p introduced in (2.3).

In what follows it is convenient to Fourier transform into momentum space. Since we are interested in studying the chiral phase transition we extend the effective action to finite temperature T and quark chemical potential μ using the Matsubara formalism.

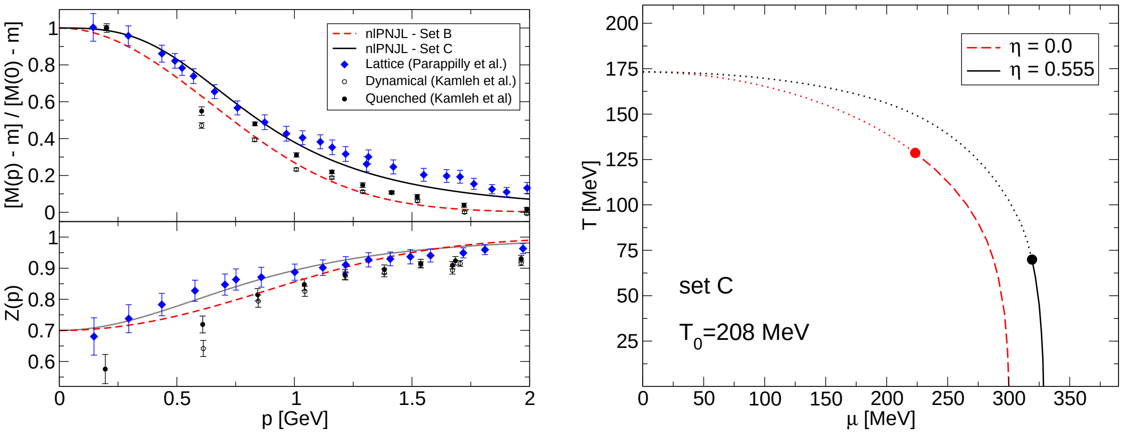

Figure 1: (Color online) Left: Normalized dynamical masses and wave function renormalization for the choice of form factors used in this study (set C), fitted to lattice data of Ref. [28] according to [27]. For comparison, more recent data [29] and alternative formfactors according to set B of Ref. [16] are shown. Right: The phase diagram of the nl-PNJL in meanfield approximation for the formfactor parametrization of set C, see also Ref. [20]. Reproducing the slope of the pseudocritical temperature $\kappa = 0.059$ from lattice QCD for small chemical potentials [19] requires a scaled vector coupling $\eta = 0.555$.

Concerning the gluon fields we use the same prescription as in previous works [14, 16], but in our present case we have chosen a μ-dependent logarithmic effective potential described in [24]

$$\mathscr{U}(\Phi,T,\mu) = (a_0 T^4 + a_1\mu^4 + a_2 T^2\mu^2)\Phi^2 + a_3 T_0^4 \ln\left(1 - 6\Phi^2 + 8\Phi^3 - 3\Phi^4\right) , \qquad (2.4)$$

where $a_0 = -1.85$, $a_1 = -1.44\times 10^{-3}$, $a_2 = -0.08$, $a_3 = -0.40$. In the present work we set the T_0 parameter by using the value corresponding to two flavours $T_0 = 208$ MeV, as it has been suggested in [25], and used in subsequent approaches, including the nonlocal PNJL [26] and Polyakov loop-DSE models [17].

Finally, to fully specify the nonlocal models under consideration we fix the model parameters as well as the form factors $g(q)$ and $f(q)$ following [16, 27], from where we choose the more realistic combination of Lorentzian functions (set C, according to the notation in Ref. [16]). These form factors have been chosen [27] such as to reproduce the dynamical mass function $M(p)$ and the WFR $Z(p)$ from lattice QCD simulations of the quark propagator in the vacuum [28], shown in the left panel of Fig. 1. For comparison, also the more recent data [29] and alternative formfactors according to set B of Ref. [16] are shown.

Within this framework the mean field thermodynamical potential $\Omega^{\rm MFA}$ results

$$\Omega^{\rm MFA} = -4T\sum_{n,c}\int\frac{d^3\vec{p}}{(2\pi)^3}\ln\left[\frac{(\tilde{\rho}^c_{n,\vec{p}})^2 + M^2(\rho^c_{n,\vec{p}})}{Z^2(\rho^c_{n,\vec{p}})}\right] + \frac{\sigma_1^2+\kappa_p^2\,\sigma_2^2}{2G_S} - \frac{\omega^2}{2G_V} + \mathscr{U}(\Phi,T) , \quad (2.5)$$

where $M(p)$ and $Z(p)$ are given by

$$M(p) = Z(p)\left[m + \sigma_1\, g(p)\right] , \quad Z(p) = \left[1 - \sigma_2\, f(p)\right]^{-1} . \qquad (2.6)$$

In addition, as in [16], we have considered

$$\left(\rho^c_{n,\vec{p}}\right)^2 = \left[(2n+1)\pi T - i\mu + \phi_c\right]^2 + \vec{p}^{\,2} , \tag{2.7}$$

where the quantities ϕ_c are given by the relation $\phi = \mathrm{diag}(\phi_r, \phi_g, \phi_b)$. Namely, $\phi_c = c\ \phi_3$ with $c = 1, -1, 0$ for r, g, b, respectively. In the case of $\left(\tilde{\rho}^c_{n,\vec{p}}\right)$ we have used the same definition as in (2.7) but shifting the chemical potential according to

$$\tilde{\mu} = \mu\ - \omega\, g(p)\, Z(p) . \tag{2.8}$$

The expression for Ω^{MFA} as given in (2.5) turns out to be divergent and, thus, needs to be regularized. For this purpose we use the same prescription as in [16, 30]. A necessary condition to find the set of mean field values for $\sigma_{1,2}$, ω and ϕ_3 which would correspond to the absolute minimum of the regularized thermodynamic potential is the fulfillment of the coupled "gap" equations

$$\frac{\partial\Omega^{\mathrm{MFA}}_{\mathrm{reg}}}{\partial\sigma_1} = \frac{\partial\Omega^{\mathrm{MFA}}_{\mathrm{reg}}}{\partial\sigma_2} = \frac{\partial\Omega^{\mathrm{MFA}}_{\mathrm{reg}}}{\partial\omega} = \frac{\partial\Omega^{\mathrm{MFA}}_{\mathrm{reg}}}{\partial\phi_3} = 0 . \tag{2.9}$$

Two of these meanfields are regarded as order parameters as their nonvanishing value signals the breaking of a symmetry in the system: the quark mass gap σ_1 stands for the breaking of the chiral symmetry and the traced Polyakov loop $\Phi = [1 + 2\cos(\phi_3/T)]/3$ signals the SU(3) center symmetry breaking signalling deconfinement. In the right panel of Fig. 1 we show the phase diagram of the chiral transition in the $T - \mu$ plane for two values of the scaled vector coupling $\eta = G_V/G_S$. The dotted lines show the pseudocritical temperatures of the chiral crossover transition which at the critical endpoints (CEP), shown as filled circles, go over to the critical temperatures (dashed and solid lines) of the first order transition where the chiral order parameter is discontinuous. Within the set C parametrization the value $\eta = 0.555$ is required for reproducing the slope of the pseudocritical temperature $\kappa = 0.059$ obtained in LQCD simulations for small chemical potentials [19]. In comparison to a vanishing, or lower, vector coupling the CEP is situated at a lower temperature and higher chemical potential. The CEP position also depends on the parametrization of the PNJL model. In the local limit it even vanishes, see Ref. [20] for details.

The EoS for quark matter is then obtained from

$$P(T,\mu) = -\min_{\sigma_1,\sigma_2,\omega,\phi_3} \Omega^{\mathrm{MFA}}_{\mathrm{reg}}(T,\mu;\{\sigma_1,\sigma_2,\omega,\phi_3\}) , \tag{2.10}$$

which holds for a homogeneous system. On the left panel of Fig. 2 we show the $T = 0$ EoS of the nl-PNJL model in set C parametrization for different values of η.

3. Deconfinement phase transition in compact stars

The deconfinement phase transition between nuclear matter and quark matter under compact star conditions[1] is constructed by solving the corresponding condition for phase equilibrium

$$P_Q(\mu_c) = P_H(\mu_c) , \tag{3.1}$$

[1]Here we consider local charge neutrality and $\beta-$ equilibrium. A more elaborated treatment considers finite size structures ("pasta") in the mixture of hadronic and quark matter. See [31] for a recent discussion and references.

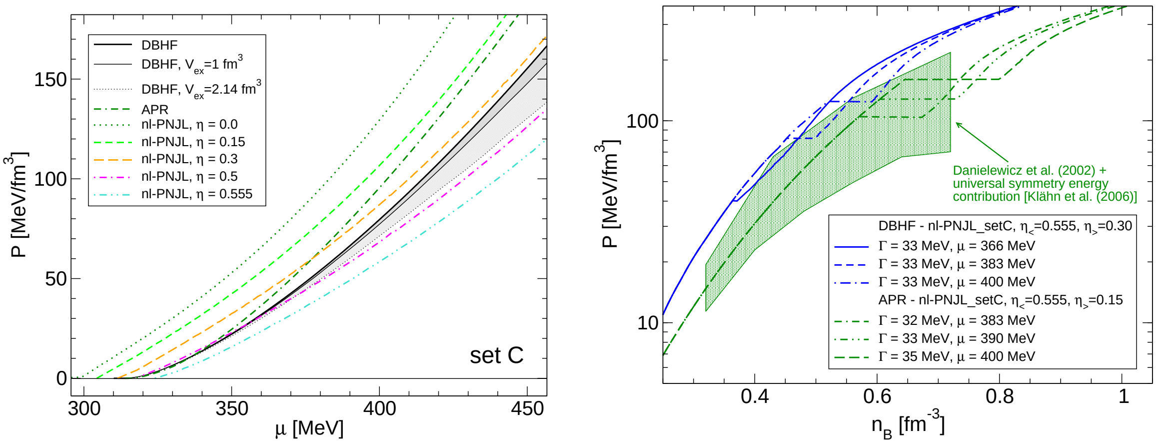

Figure 2: (Color online) Left: Pressure vs. baryochemical potential EoS for neutron star matter in the hadronic phase (DBHF with and without excluded volume $V_{\rm ex}$, APR) compared to that of the quark matter phase (nl-PNJL) for different values of η. For $\eta \gtrsim 0.5$ nuclear matter is stable at low densities. For a phase transition to quark matter at high densities (chemical potentials) the vector coupling has to get reduced to a value $\eta_> \lesssim 0.3$. Right: Hybrid EoS, where the quark sector is provided using the interpolation (3.2) and two alternatives for hadronic phase are used (APR and DBHF). The phase transition from hadronic to quark matter is determined by Eq. (3.1). The green hatched area corresponds to the EoS constraint for symmetric matter from the flow data analysis [35] shifted by the universal symmetry energy contribution [36].

where μ_c is the critical chemical potential for the transition. The index H stands for "hadronic" and here we will use one of the standard nuclear matter EoS: APR [32] or DBHF [33]. The index Q stands for "quark" and the corresponding EoS will be introduced based on the following discussion. Inspecting the left panel of Fig. 2, we observe that choosing for $P_Q(\mu) = P(0,\mu)$, i.e. the EoS (2.10) for the nl-PNJL with a constant vector coupling strength η there occurs one of the following problems: (a) quark matter is favorable for all chemical potentials, even at lowest densities (for $\eta \lesssim 0.3$); (b) nuclear matter is favorable for all chemical potentials, even at highest densities (for $\eta \gtrsim 0.5$); (c) quark and hadronic EoS cross each other either in the "wrong" way (confinement at high densities) or more than once (for $\eta \sim 0.4 \ldots 0.5$) since they are marginally indistinguishable in the relevant range of chemical potentials. The latter situation has been called the "masquerade" problem [34].

In this situation we suggest the following procedure to avoid unphysical solutions and the masquerade problem. We anticipate a chemical potential dependence of the scaled vector coupling, $\eta(\mu)$, in such a way that at low chemical potentials the value $\eta_< = 0.555$ is set which is necessary to reproduce the slope of the pseudocritical temperature and at high chemical potentials, beyond a fiducial range for the deconfinement transition, an asymptotic value is attained which makes the quark matter EoS favorable over the hadronic one under consideration. For $H =$ DBHF, this is $\eta_> \leq 0.3$. For the transition between both regions we suggest here an interpolation ansatz

$$P_Q(\mu) = P(0,\mu;\eta_<)f_<(\mu) + P(0,\mu;\eta_>)f_>(\mu) \,, \tag{3.2}$$

$$f_{\lessgtr}(\mu) = \frac{1}{2}\left[1 \mp \tanh\left(\frac{\mu-\bar{\mu}}{\Gamma}\right)\right] \,. \tag{3.3}$$

For the two free parameters of the interpolation we suggest the ranges $\bar{\mu} \sim 360 \ldots 410$ MeV and

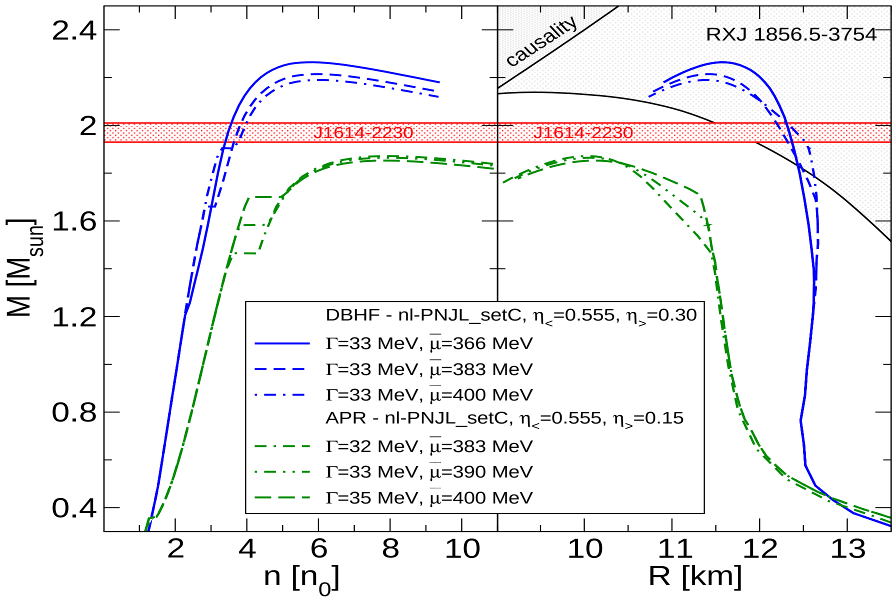

Figure 3: (Color online) Hybrid star sequences based on the DBHF and APR EoS for nuclear matter and the nl-PNJL model for quark matter proposed here, shown together with constraints on the maximum mass from PSR J1614-2230 [1] and on the mass-radius relation from RX J1856.5-3754 [39].

$\Gamma \sim 30$ MeV. The motivation of this choice comes from considering the influence of a nucleonic excluded volume, shown also in the left panel of Fig. 2, which stems from the quark Pauli blocking between nucleons and thus estimates the onset of quark substructure effects like the overlap of hadronic wave functions in dense matter modifying effective quark-meson couplings.

Two sets of resulting hybrid EoS, based on DBHF and APR as hadronic EoS, respectively, are obtained by the Maxwell construction according to Eq. (3.1). They are shown on the right panel of Fig. 2 together with a constraint for compact star EoS obtained from the flow data analysis for symmetric matter [35] shifted by a contribution due to the universal symmetry energy of Ref. [36].

With these hybrid EoS the Tolman–Oppenheimer–Volkoff equations [37, 38] have been solved and the resulting sequences of nonrotating compact star configurations have been obtained. The corresponding dependencies of the mass M of the stars on their radius R and on their central density $n(0)$ are shown the left and right panels of Fig. 3, respectively.

The hybrid star sequences based on the APR EoS do not fulfill the constraint on the maximum mass from the mass measured for PSR J1614-2230 [1] and also do not obey the constraint on the minimal radius for a given mass from RX J1856.5-3754 [39] since these hybrid EoS describe too "soft" compact star matter [2]. The hybrid stars based on the DBHF EoS fulfill both constraints and, depending on the specific $\mu-$ dependence of the vector coupling strength $\eta(\mu)$, can have an onset of quark matter in their interiors already at a mass as low as 1.2 $M_{\odot}$. This would include

[2]Note that the analysis of X-ray burst sources in Ref. [40] can provide at best a lower limit on the star radius which is embedded in that for RX J1856.5-3754, see Ref. [41] for a discussion.

all compact stars with measured masses known so far. However, these EoS are too stiff for the constraint from flow data [35] combined with the universal symmetry energy contribution [36].

4. Results and Conclusions

A nonlocal Polyakov-NJL model with vector meson meanfield has been calibrated with lattice QCD data for the momentum dependence of the wave function renormalization and dynamical mass of the quark propagator in vacuum as well as for the slope of the pseudocritical temperature at small chemical potentials which fixes the vector coupling strength under these conditions.

A straightforward application to nonzero temperatures and chemical potentials within the Matsubara formalism results in a prediction for the position of the critical endpoint.

Considering compact star matter at $T = 0$ results in the conclusion that quark matter in compact stars cannot occur since its pressure stays always below that of standard hadronic EoS for all relevant baryon densities, unless a medium dependence of basic nl-PNJL model parameters is invoked. A generic ansatz for the chemical potential dependence of the vector coupling strength is presented which allows to estimate the ballpark for such a dependence allowing hybrid star configurations which fulfill basic compact star constraints. Examples illustrate the sensitivity to the nuclear EoS: While the set of hybrid star EoS based on APR is too soft to fulfill mass and radius constraints, those based on DBHF satisfy these constraints but appear too stiff for the flow data from heavy-ion collisions. Thus compact star observations and heavy-ion collisions together may guide the path towards the EoS of dense QCD matter.

Acknowledgement

The authors acknowledge support from CompStar, a Research Networking Programme of the European Science Foundation and the programme of the Polish Ministry for Science and Higher Education for supporting it. D.B. profited from inspiring discussions with Tetsuo Hatsuda, Ken-Ichi Imai, Toshiki Maruyama, Kota Masuda, Thomas Rijken, Tatsuyuki Takatsuka, Nobutoshi Yasutake at the J-PARC workshop and the SNP school during his visit at the Research Group for Hadron Physics at the Advanced Sciene Research Center of JAEA in Tokai where this work was completed. He is grateful for financial support from RFFI under grant number 11-02-01538a and the JAEA Foreign Researcher Inviting Program. D.B. and D.E.A.C. were supported by the Polish National Science Center under the “Maestro” programme. S.B. acknowledges support of the Croatian Ministry of Science, Education and Sports under contract No. 119-0982930-1016. R.Ł. received support from the faculty of Physics and Astronomy at the University of Wrocław under grant number 2291/M/IFT/12.

References

[1] P. Demorest, T. Pennucci, S. Ransom, M. Roberts and J. Hessels, Nature **467**, 1081 (2010).

[2] V. A. Ambartsumyan and G. S. Saakyan, Soviet Astronomy **4**, 187 (1960).

[3] G. Baym and S. A. Chin, Phys. Lett. B **62**, 241 (1976).

[4] M. Alford *et al.*, Nature **445**, E7 (2007).

[5] T. Klähn *et al.*, Phys. Lett. B **654**, 170 (2007).
[6] F. Özel, D. Psaltis, S. Ransom, P. Demorest, M. Alford, ApJ **725**, 1918 (2010).
[7] T. Klähn, D. Blaschke and R. Łastowiecki, Acta Phys. Polon. Supp. B **5**, 757 (2012).
[8] S. Weissenborn, I. Sagert, G. Pagliara, M. Hempel and J. Schaffner-Bielich, ApJ **740**, L14 (2011).
[9] I. Bednarek, P. Haensel, J. L. Zdunik, M. Bejger and R. Manka, A& A **543**, A157 (2012).
[10] R. Lastowiecki, D. Blaschke, H. Grigorian and S. Typel, Acta Phys. Polon. Supp. **5**, 535 (2012).
[11] T. Klähn, PoS QNP **2012**, 029 (2012).
[12] A. Sedrakian, arXiv:1301.2675 [astro-ph.HE].
[13] D. Blaschke, M. Buballa, A. E. Radzhabov and M. K. Volkov, Yad. Fiz. **71**, 2012 (2008).
[14] G. A. Contrera, D. Gomez Dumm and N. N. Scoccola, Phys. Lett. B **661** (2008) 113.
[15] T. Hell, S. Roessner, M. Cristoforetti and W. Weise, Phys. Rev. D **79** (2009) 014022.
[16] G. A. Contrera, M. Orsaria and N. N. Scoccola, Phys. Rev. D **82**, 054026 (2010).
[17] D. Horvatic, D. Blaschke, D. Klabucar and O. Kaczmarek, Phys. Rev. D **84**, 016005 (2011).
[18] T. Hell, K. Kashiwa and W. Weise, Phys. Rev. D **83**, 114008 (2011).
[19] O. Kaczmarek *et al.*, Phys. Rev. D **83**, 014504 (2011).
[20] G. A. Contrera, A. G. Grunfeld and D. B. Blaschke, arXiv:1207.4890 [hep-ph].
[21] T. Hell, K. Kashiwa and W. Weise, arXiv:1212.4017 [hep-ph].
[22] D. B. Blaschke *et al.*, Phys. Rev. C **75**, 065804 (2007).
[23] M. Orsaria, H. Rodrigues, F. Weber and G. A. Contrera, Phys. Rev. D **87**, 023001 (2013).
[24] V. A. Dexheimer and S. Schramm, Phys. Rev. C **81**, 045201 (2010).
[25] B. J. Schaefer, J. M. Pawlowski and J. Wambach, Phys. Rev. D **76**, 074023 (2007).
[26] V. Pagura, D. Gómez Dumm and N. N. Scoccola, Phys. Lett. B **707**, 76 (2012).
[27] S. Noguera and N. N. Scoccola, Phys. Rev. D **78**, 114002 (2008).
[28] M. B. Parappilly *et al.*, Phys. Rev. D **73**, 054504 (2006).
[29] W. Kamleh *et al.*, Phys. Rev. D **76**, 094501 (2007).
[30] D. Gomez Dumm and N. N. Scoccola, Phys. Rev. C **72**, 014909 (2005).
[31] N. Yasutake, T. Noda, H. Sotani, T. Maruyama and T. Tatsumi, arXiv:1208.0427 [astro-ph.HE].
[32] A. Akmal, V. R. Pandharipande and D. G. Ravenhall, Phys. Rev. C **58**, 1804 (1998).
[33] E. N. E. van Dalen, C. Fuchs and A. Faessler, Nucl. Phys. A **744**, 227 (2004).
[34] M. Alford, M. Braby, M. W. Paris and S. Reddy, ApJ **629**, 969 (2005).
[35] P. Danielewicz, R. Lacey and W. G. Lynch, Science **298**, 1592 (2002).
[36] T. Klähn *et al.*, Phys. Rev. C **74**, 035802 (2006).
[37] R. C. Tolman, Phys. Rev. **55**, 364 (1939).
[38] J. R. Oppenheimer and G. M. Volkoff, Phys. Rev. **55**, 374 (1939).
[39] J. E. Trümper, V. Burwitz, F. Haberl and V. E. Zavlin, Nucl. Phys. Proc. Suppl. **132**, 560 (2004).
[40] A. W. Steiner, J. M. Lattimer and E. F. Brown, Astrophys. J. Lett. **765**, L5 (2013).
[41] J. Trümper, Prog. Part. Nucl. Phys. **66**, 674 (2011).